JMEPEG (2006) 15:122-129
DOI: 10.1361/105994906X83402

1059-9495/$19.00

Performance of High-Velocity Oxyfuel-Sprayed Coatings on an Fe-Based Superalloy in Na_2SO_4-60%V_2O_5 Environment at 900 °C Part I: Characterization of the Coatings

T.S. Sidhu, S. Prakash, and R.D. Agrawal

(Submitted May 25, 2005; in revised form August 9, 2005)

This article demonstrates the successful formulation of NiCrBSi, Cr_3C_2-NiCr, Ni-20Cr, and Stellite-6 coatings on an Fe-based superalloy by a high-velocity oxyfuel (HVOF) process for hot corrosion applications. The microstructure, porosity, coating thickness, phase formation, and microhardness properties of the coatings have been characterized using the combined techniques of optical microscopy, x-ray diffraction, scanning electron microscopy/energy-dispersive x-ray analysis. A microhardness tester was used to determine the hardness of the coatings. The coatings in general exhibit characteristic splat-like, layered morphologies due to the deposition and resolidification of successive molten or semimolten powder particles. The NiCrBSi, Cr_3C_2-NiCr, and Ni-20Cr coatings have shown a nickel-base face-centered cubic (fcc) structure as a principal phase, whereas Stellite-6 coating has an fcc Co-rich metallic matrix. Oxides/spinel oxides are formed in small fraction as intersplat lamellae or globules oriented parallel to the substrate surface. Coatings possess some unmelted/partially melted particles, inclusions, and porosity less than 2%. The microhardness of the coatings is found to be higher than the superalloys. The Cr_3C_2-NiCr coating has indicated a maximum microhardness of 990 Hv, while a Ni-20Cr coating has shown a minimum value of about 600 Hv. This article is focused on the characterization of HVOF coatings. The hot corrosion behavior of these coatings in a molten salt (Na_2SO_4-60%V_2O_5) environment at 900 °C under cyclic conditions is being presented as part II included in this issue.

Keywords high-velocity oxyfuel process, hot corrosion, protective coatings, superalloy

1. Introduction

Superalloys have been developed for high-temperature applications, but they are not able to meet the simultaneous goals of high-temperature strength and high-temperature corrosion resistance, so protective coatings on superalloys are used to counter the latter (Ref 1). Coatings provide a way of extending the limits of use of materials at the upper end of their performance capabilities by allowing the mechanical properties of the substrate materials to be maintained while protecting them against wear or corrosion (Ref 2). Coatings can aggregate value to products up to 10 times their cost (Ref 3).

Coatings can be produced by thermal spraying (vacuum plasma spraying [VPS], low-pressure plasma spraying [LPPS], and high-velocity oxyfuel [HVOF]) by sputtering or by evaporation; however, generally for industrial applications, thermally sprayed coatings are preferred (Ref 4, 5). Whereas thermal sprayed coatings have limited usefulness as corrosion protection coatings due to the presence of interconnected porosity in the structure. However, with the advent of the HVOF process, the coatings deposited by this technique are being studied extensively for their corrosion-resistant properties (Ref 6). The HVOF process is now widely used to deposit various types of coatings, which have low porosity and high hardness, and are relatively well-bonded to the substrate being protected (Ref 5, 7-10). In recent years, there has been a considerable growth in the use of this spraying process to deposit cermets, metallic and ceramic protective overlay coatings, which are typically 100 to 300 μm thick, onto the surfaces of engineering components to allow them to function under extreme conditions (Ref 7, 11). So far, several HVOF spraying coatings have been subjected to the corrosion test in seawater. In addition to the cermets (Ref 12-14), the anticorrosion alloys (Ref 15-17) were adopted as the coating materials. These studies concluded that the HVOF method is superior to other spraying techniques for depositing coatings having higher corrosion resistance. The HVOF coatings have formed many industrial applications in petrochemical and offshore industries, automotive components and general engineering applications (Ref 18). Therefore, in this study, the HVOF process has been selected to deposit the coatings.

The composition and structures of the coatings are determined by the role that they have to play in the various material systems and performance environments (Ref 19). The coating should have a composition that will react with the environment to produce the most protective scale possible, to provide corrosion resistance with long-term stability, and to have resistance to cracking or spallation under mechanical and thermal stresses induced during the operation of the component (Ref 20).

There is an increasing interest in the deposition of Ni-base metallic alloys for protection against corrosion. Nickel-

T.S. Sidhu, S. Prakash, and **R.D. Agrawal,** Metallurgical & Materials Engineering Department, Indian Institute of Technology Roorkee, Roorkee-247 667, India. Contact e-mail: tssidhu@rediffmail.com.

Table 1 Composition of the coating alloys, coating thickness, and porosity

Coating alloys	Chemical composition, wt.%	Particle size and shape	Coating thickness, μm	Porosity, %age
Cr_3C_2-NiCr Powder (LA-6875), Blend of 75%LA-6304 and 25% LA-7319	75Cr_3C_2-25 (Ni-20Cr)	−45 μm + 5 μm, irregular	290	<1.8%
NiCrBSi Powder (PA 101HV)	Ni-15.3Cr-3.1B-4.8Si-4.2Fe-0.6C	−45 μm, spherical	285	<1.4%
Stellite-6 Powder (Jet-Kote 7206)	Co-1.2C-28Cr-4.9W-2.7Fe-2.3Ni-1.1Si	−45 μm, spherical	298	<1.9%
Ni-20Cr wire	Ni-20Cr	Wire diameter 3.17 mm	236	<1%

chromium alloys have been used as coatings to deal with oxidation and corrosive environments at high temperature. When nickel is alloyed with chromium, this element oxidizes to protective surface oxide Cr_2O_3 at rates that could make it suitable for use up to about 1473 K (Ref 21, 22). Further, for high-temperature applications requiring wear resistance, thermally sprayed (Cr_xC_y-NiCr) coatings are used in light of the excellent corrosion and oxidation resistance of the nickel-chromium alloy and reasonable wear resistance of chromium carbides at temperatures up to 900 °C (Ref 23). The largely used Ni-base powder belongs to the Ni-B-Si system, with the addition of other alloying elements (Ref 24, 25). Cobalt-base alloys containing chromium, tungsten, and carbon, known as Stellite-6, has high hardness at high temperature, high corrosion resistance, and wear resistance (Ref 26, 27).

The objective of the present research work is to characterize the HVOF-sprayed NiCrBSi, Cr_3C_2-NiCr, Ni-20Cr, and Stellite-6 coatings deposited on an Fe-base superalloy, because it is essential to evaluate the hot corrosion behavior of these coatings for specific applications in energy conversion systems. The hot corrosion behavior of these coatings in a molten salt (Na_2SO_4-60%V_2O_5) environment is being presented in part II. The superalloy selected for this study has been provided by Mishra Dhatu Nigam Limited (Hyderabad, India) to find suitable protective coatings for extending the life of the superalloy at the upper end of their performance capabilities. The microstructure, porosity, coating thickness, phase formation, and microhardness properties of the coatings have been characterized using the combined techniques of optical microscopy, x-ray diffraction (XRD), scanning electron microscopy (SEM)/energy-dispersive x-ray analysis (EDAX).

2. Experimental Procedure

2.1 Development of Coatings

2.1.1 Substrate Material. The Fe-based superalloy Superfer 800H, which was developed by M/S Mishra Dhatu Nigam Limited (Hyderabad, India), was used as a substrate material. This superalloy is used in steam boilers, furnace equipment, heat exchangers, and piping in the chemical industry, and reformer, baffle plates/tubes in fertilizer plants. The chemical composition of the Superfer 800H is 32Ni-21Cr-0.3Al-0.3Ti-1.5Mn-1.0Si-0.1C-balance Fe. Specimens with dimensions of approximately 20 × 15 × 5 mm were cut from the alloy sheet, were polished with SiC papers down to 180 grit, and subsequently were grit-blasted with alumina powders (Grit 45) before development of the coatings by the HVOF process.

2.1.2 Coating Formulation. Four types of commercially available coating alloys (Cr_3C_2-NiCr, NiCrBSi, and Stellite-6 in the powder form, and Ni-20Cr in the wire form) were used in the study. Details of these coating alloys are given in Table 1. As evident from the micrographs of the coating powders shown in Fig. 1, Cr_3C_2-NiCr powder particles have an irregular shape, whereas NiCrBSi and Stellite-6 powders have a spherical morphology. A wide particle size range of all the coating powders is found to be consistent with the nominal size provided by the manufacturer.

The coatings were developed at M/S Metallizing Equipment Co. Pvt. Ltd. (Jodhpur, India) by using two types of commercial HVOF thermal spray systems. The Hipojet-2100 HVOF system was used for powder spraying, and the Hijet-9600 HVOF system was used for wire spraying. Liquefied petroleum gas (LPG) was used as a fuel. All of the process parameters were kept constant throughout the coating process. The specimens were cooled with compressed air jets during and after spraying. The spray parameters used for the Hipojet-2100 system were an oxygen flow rate of 250 L/min (LPM), a fuel (LPG) flow rate 60 LPM, an airflow rate of 900 LPM, a spray distance of about 200 mm, a fuel pressure of 6 kg/cm^2, an oxygen pressure of 8 kg/cm^2, and air pressure 6 kg/cm^2. The spray parameters used for the Hijet-9600 system were the same except for an oxygen flow rate of 200 LPM, a fuel (LPG) flow rate of 50 LPM, a fuel pressure of 4 kg/cm^2, and an oxygen pressure 6 kg/cm^2.

2.2 Characterization of the Coatings

The coated samples were cloth wheel-polished and then subjected to optical microscopy, XRD, and SEM/EDAX analysis to characterize the surface and cross-sectional morphology of the coatings. A Axiovert 200 MAT (Zeiss, New York) inverted optical microscope, fitted with imaging software (Axiovision Release 4.1, Zeiss), was used for optical microscopy. The XRD analysis was carried out with a Bruker AXS D-8 Advance Diffractometer (Germany) with CuKα radiation. A scanning electron microscope (JSM-5800, Jeol, New York) with an EDAX attachment (model 6841, Oxford, UK) was used for SEM/EDAX analysis. The porosity measurements were made with an image analyzer having Dewinter Material Plus 1.01 software based on ASTM standard B276. The image was obtained through the attached PMP3 inverted metallurgical microscope. To identify the cross-sectional details, the samples were cut across the cross section, mounted in transoptic powder, and subjected to mirror polishing. The coating thickness was measured by obtaining a backscattered electron image (BSEI) with a scanning electron microscope (LEO 435VP), which was attached to a Robinson Back Scattered Detector. The microhardness of coatings was measured by the Leitz Hardness Tester Miniload 2. A 15 g (147.1 mN) load was provided to the needle because the penetration and hardness value was based on the relation $Hv = 1854.4 \times F/d^2$ (where F is the load in grams and d is the mean penetrated diameter in micrometers).

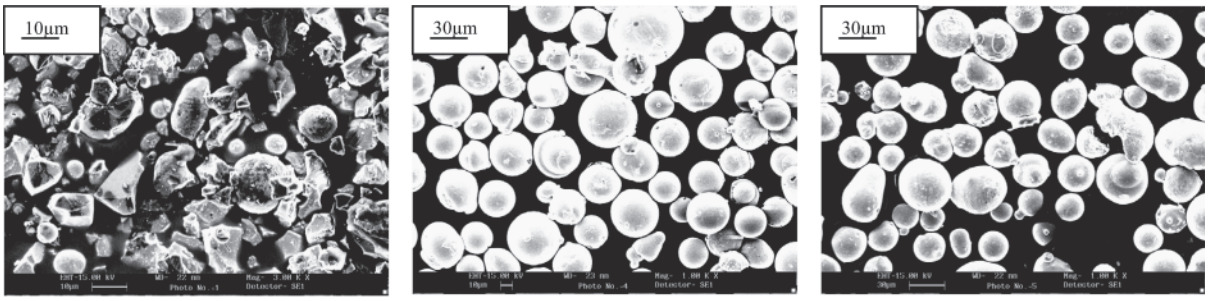

Fig. 1 SEM of different coating powders: (a) Cr_3C_2-NiCr powder; (b) NiCrBSi powder; and (c) Stellite-6 powder

3. Results

3.1 Measurement of Coating Thicknesses

The thickness of the coatings has been measured from the BSEI obtained from along the cross section of the mounted samples. The BSEI for the coatings have been shown in Fig. 2. The thickness of the coatings, as measured from the BSEI, has been reported in the Table 1. The thickness of the coatings has been found to be in the range of 250 to 300 μm.

3.2 Porosity of the Coatings

The porosity of the coatings has a significant role to play as far as the corrosion resistance of thermal spray coatings is concerned. Dense coatings usually provide better corrosion resistance than the porous coatings. Porosity measurements were made for the HVOF-sprayed coatings, which are found to be less than 2%, and the values are shown in Table 1.

3.3 Cross-Sectional Morphology of the Coatings

The coatings have been deposited on a stationary substrate by moving the HVOF gun, and the required thickness of the coatings has been obtained by varying the number of passes. This led to the development of a lamellar structure in the coatings, as is evident from the micrographs in Fig. 2 and 3. Some unmelted/partially melted particles and inclusions have been observed in the structure. All of the coatings have a dense structure with the porosity (less than 2%) randomly distributed in the coatings. Oxides, which are believed to be formed as a result of the oxidation of in-flight particles between successive runs, have appeared in the microstructure in the form of intersplat lamellae or globules that are oriented parallel to the substrate surface. Some dark spots that appeared in the structure of the coatings or at the coating-substrate interface may be the inclusions.

3.4 Surface Morphology of the Coatings

Figure 4 depicts the optical micrographs of the surface of the coatings. It can be observed from the microstructures that coatings in general possess some porosity, inclusions, and partially melted particles. Cr_3C_2-NiCr and Ni-20Cr wire coatings have almost uniformly distributed irregularly shaped fine-grain microstructures, whereas the Stellite-6 coating has a regularly sized globular morphology. Some unmelted particles are also observed in the structure of as-sprayed Cr_3C_2-NiCr coatings as well as Stellite-6 coatings (Fig. 4a, c). Unmelted particles are identified in the coating by their size and surface morphology. The structure of the as-sprayed NiCrBSi coating mainly consists of a γ nickel solid solution (Ref 28). Contrast black spots in the coating structure indicate porosity, and dark black areas may be the inclusions. Thin contrast stringers appearing in the microstructure are presumably the oxide (Fig. 4c), as identified by XRD analysis.

3.5 Microhardness of the Coatings

The microhardness data of the coatings has been compiled in Fig. 5, which shows microhardness profiles along the cross section of the coatings as a function of distance from the coating-substrate interface. The microhardness of the substrate has been found to be in the range of 250 to 340 Hv. As indicated by the profiles, the maximum value of the hardness has been achieved by Cr_3C_2-NiCr coating of the order of 990 Hv, whereas a minimum of 600 Hv has shown by the Ni-20Cr wire coating. Further, an increase in the microhardness of the substrate has been observed near the coating-substrate interface in all cases (see points at a distance of −40 μm).

3.6 X-Ray Diffraction Analysis

X-ray diffractograms, as shown in Fig. 6, indicate that Cr_3C_2-NiCr, NiCrBSi, and Ni-20Cr wire coatings have a nickel-base face-centered cubic (fcc) structure as a principal phase, whereas the Stellite-6 coating has a principal phase of Cobased fcc. Very weak peaks of Cr_2O_3 oxide and $CoNiO_2$ spinel oxide phases have also been identified in the XRD patterns of the Ni-20Cr and Stellite-6 coatings, respectively. Moreover, Cr_3C_2-NiCr and NiCrBSi coatings have also indicated the presence of very low-intensity peaks of Cr_7C_3, whereas the additional Ni_3B phase is revealed by the latter.

3.7 Scanning Electron Microscopy/Energy-Dispersive X-Ray Analysis

Micrographs obtained using a scanning electron microscope of the as-coated surfaces of different coatings are given in Fig. 7. In general, these micrographs indicate that the coatings are massive and that there are no cracks in the coatings. In case of Cr_3C_2-NiCr coating, one can see melted, partially melted, and black areas. Partially melted areas have a composition of 69% chromium and 29% nickel, which is close to the composition of powder. The black area in the coating is found to be rich in nickel. In the case of the NiCrBSi coating, there are globular melted particles in the matrix of the partially melted layer.

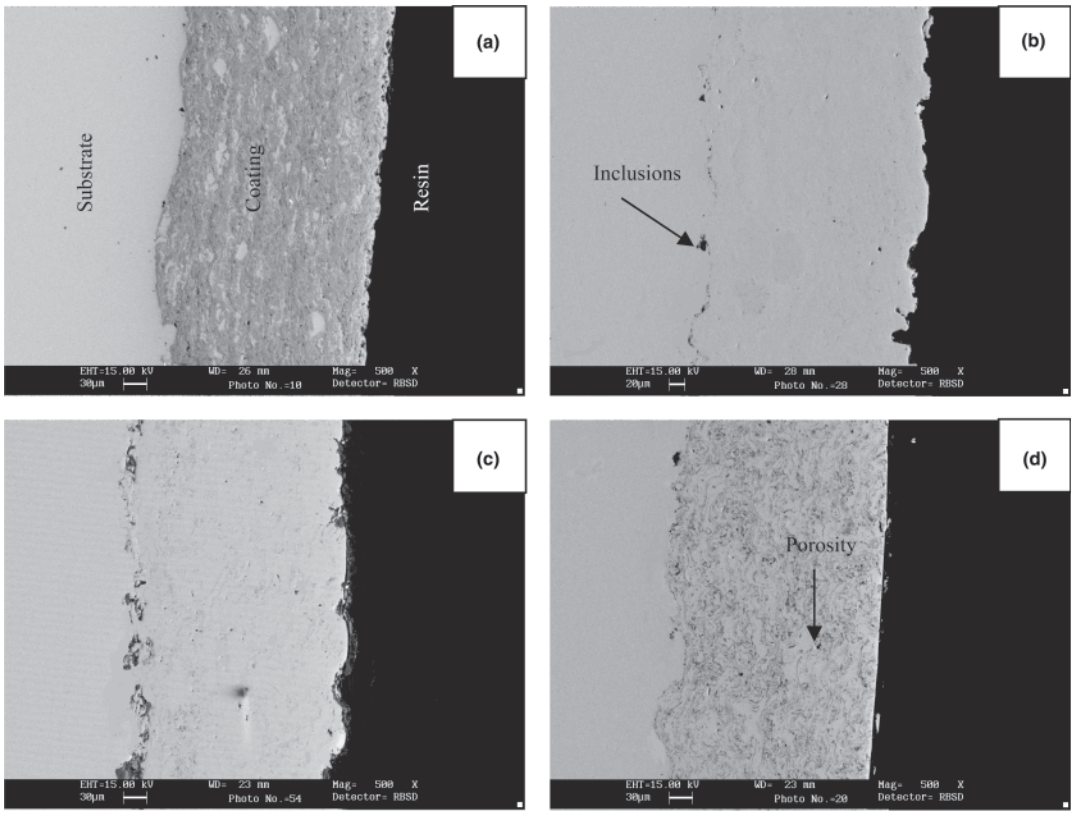

Fig. 2 BSEI showing cross-sectional morphologies of different HVOF coatings on the Superfer 800H superalloy, at a magnification of 500×: (a) Cr_3C_2-NiCr coating; (b) NiCrBSi coating; (c) Stellite-6 coating; and (d) Ni-20Cr wire coating

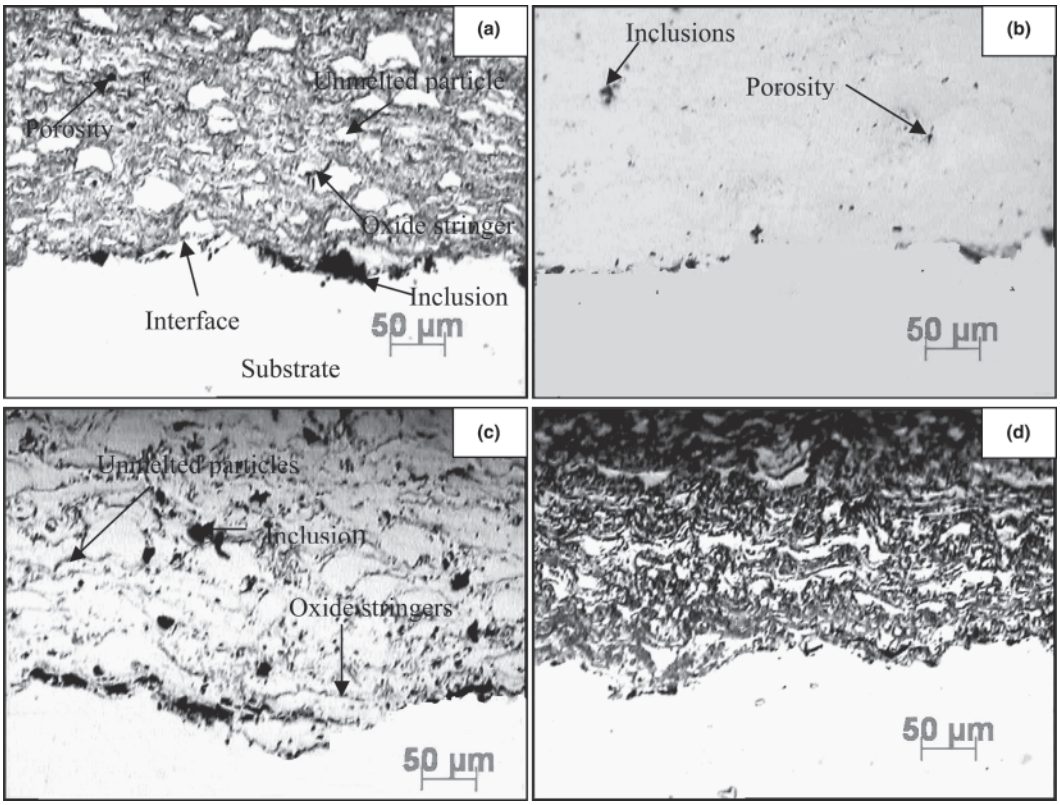

Fig. 3 Optical micrographs showing cross-sectional morphologies of different coatings on the Superfer 800H superalloy, at a magnification of 320×: (a) Cr_3C_2-NiCr coating; (b) NiCrBSi coating; (c) Stellite-6 coating; and (d) Ni-20Cr wire coating

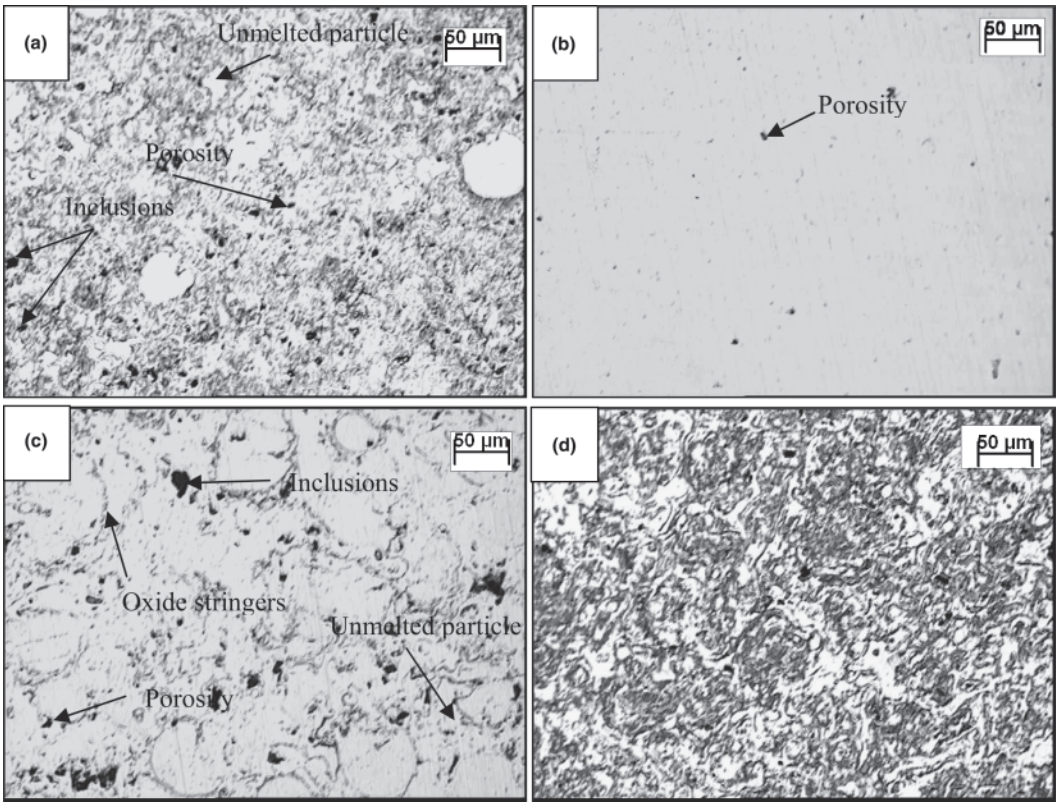

Fig. 4 Optical micrographs showing the surface morphology of different HVOF coatings on the superalloy Superfer 800H, at a magnification of 320×: (a) Cr_3C_3-NiCr coating; (b) NiCrBSi coating; (c) Stellite-6 coatings; and (d) Ni-20Cr coating

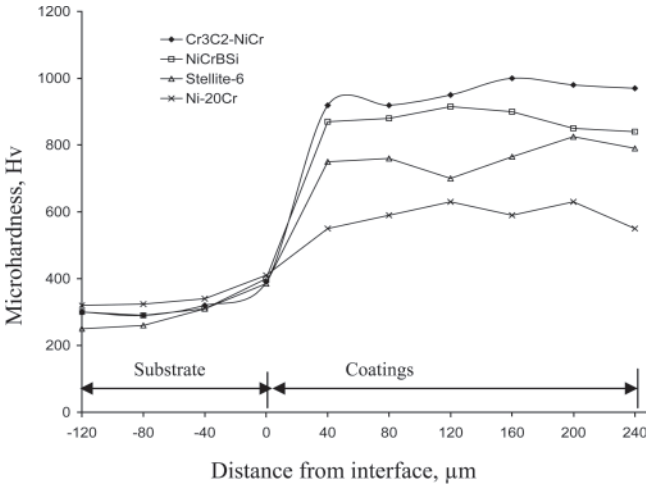

Fig. 5 Microhardness profiles of different HVOF coatings on Superfer 800H superalloy along the cross section

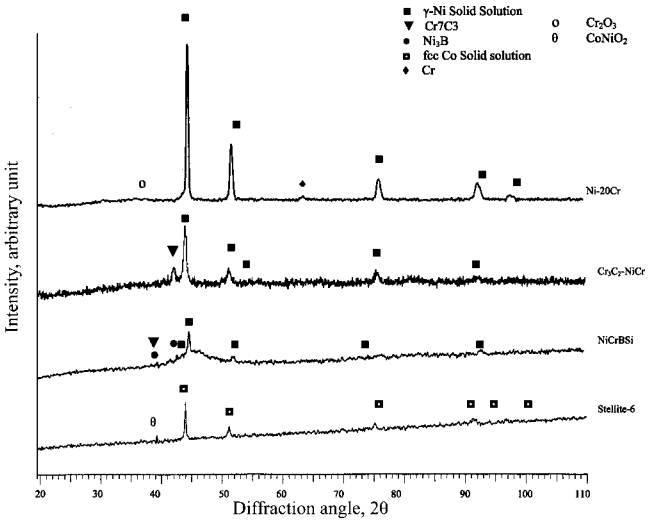

Fig. 6 The XRD analysis for the different as-sprayed coatings on the Superfer 800H superalloy

These melted particles have nearly the same composition as that of powder. Being limited by the equipment, the boron element of the coating could not be analyzed. In the case of the partially melted areas, the amount of nickel is slightly less and silicon has increased. Whereas in the case of the Stellite-6 coating, there is an indication of melted regularly sized globules, which are Co-rich splats surrounded by a partially melted zone having nearly the same composition as that of the matrix. There is a presence of unmelted particles and porosity. In the case of the Ni-20Cr wire-coated surface, one can see the melted coating having a composition similar to the wire, with some partially melted area where the nickel content is slightly higher and is depleted of chromium. In the micrographs, the regions marked "M" indicate the melted region, whereas "P" represents the partially melted/unmelted particles.

4. Discussion

The HVOF-sprayed coatings have been used for a wide range of industrial applications as this process produces uni-

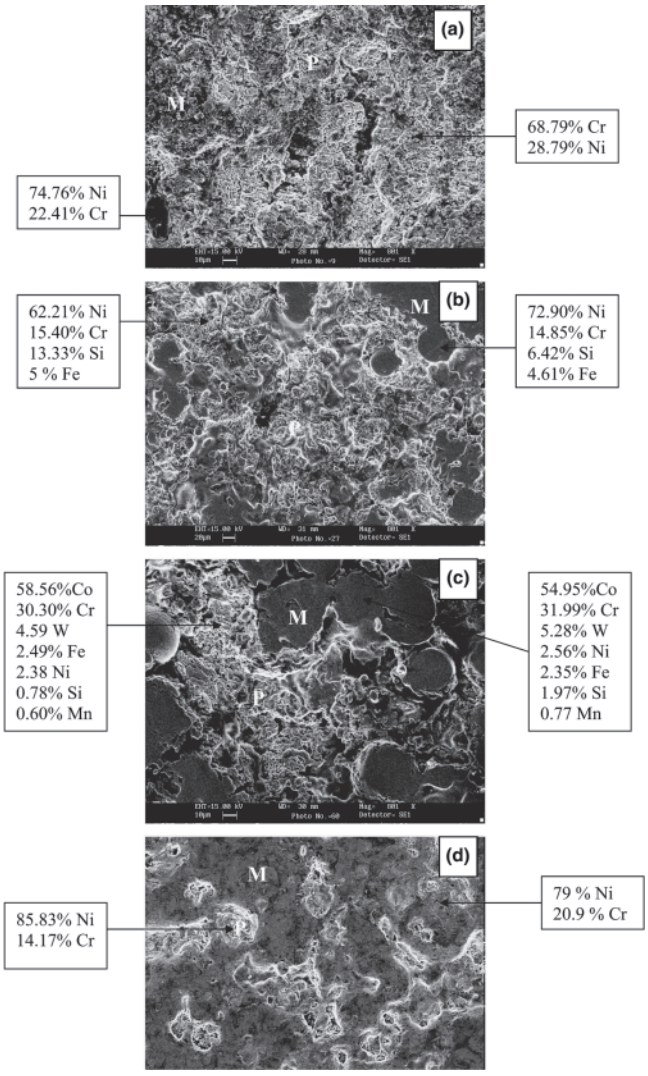

Fig. 7 A SEM/EDAX analysis of the as-sprayed coatings on the superalloy Superfer 800H, at a magnification of 800×: (a) Cr_3C_2-NiCr coating; (b) NiCrBSi coating; (c) Stellite-6 coating; and (d) Ni-20Cr wire coating

form and dense coatings, with very low porosity and high hardness values (Ref 29).

The cross-sectional morphology of the coatings shows that the coatings in general exhibit characteristic splat-like, layered morphologies due to the deposition and resolidification of molten or semimolten powder particles. The long axis of the impacted splats are oriented parallel to the substrate surfaces. Micrographs show that a high proportion of the feedstock powders/wire appear to have fully or partially melted prior to impact on the substrate, with negligible amounts of unmelted particles observed in the microstructure. Further, the coatings possess some porosity and oxide inclusions that are typical characteristics of HVOF-sprayed coatings. The microstructures observed in the current study are almost analogous with the findings of HVOF-sprayed coatings by Dent et al. (Ref 28), Kong et al. (Ref 30), Sundararajan et al. (Ref 31, 32), Ak et al. (Ref 33), and Zhao et al. (Ref 34). Some contrast stringers that have appeared in the microstructure in the form of either intersplat lamellae or globules most likely correspond to the oxide phases, which are identified as very weak peaks in the XRD spectrum. These oxides are oriented parallel to the substrate surface and are believed to be due to the oxidation of in-flight particles between successive runs. Similar findings of the formations of oxides in the HVOF coatings have also been reported by Dent et al. (Ref 28) and Sturgeon (Ref 35).

The coatings should have minimum possible porosities because they can do harm to the persistent corrosion resistance of thermal spray coatings. The porosity of the HVOF coatings has been found to be very much less. In the HVOF process, the powder particles are propelled out of the gun nozzle at high velocities toward the substrate. Due to the high velocity and high impact of the sprayed powder particles, the coatings produced by the HVOF-spraying process are very dense. The measured value of the porosity is in good agreement with the findings of Gil and Staia (Ref 36), Miguel et al. (Ref 37), Helali and Hashmi (Ref 38), and Aalamialeagha et al. (Ref 39). The coating thicknesses, as measured along the cross section for some randomly selected samples, have been found very close to the desired values.

Hardness is the most frequently quoted mechanical property of the coatings (Ref 40). The microhardness of the coatings has been found to be very high compared with the substrate superalloy (Fig. 5). The measured values of microhardness are in good agreement with the findings of Zhao et al. (Ref 34), Miguel et al. (Ref 37), Lee and Min (Ref 41), Gil and Staia (Ref 42), Wang and Lee (Ref 43), Wang and Chen (Ref 44), and Vuoristo et al. (Ref 45). The substrate near the coating interface shows a little higher value of hardness compared with the substrate. The reason for this increased hardness value near the coating-substrate interface (see points at a distance of −40 μm in Fig. 5) might be due to the work-hardening effect of the sandblasting of the substrate prior to the coating process, as suggested by Sundararajan et al. (Ref 46). This substrate hardening may also be partially attributed to the high-speed impact of the coating particles during HVOF spraying. A similar phenomenon has also been observed by Hidalgo et al. (Ref 47) and Sidhu and Prakash (Ref 48). The improved values of the hardness of the coatings in comparison with the substrate alloys is believed to be due to the high density and cohesive strength of the individual splats as a result of the high impact velocity of the coating particles, as suggested by Verdon et al. (Ref 49) and Hawthorne et al. (Ref 50).

The XRD pattern of the Cr_3C_2-NiCr coating reveals that the coating structure mainly consists of a γ nickel solid solution with very weak peaks of Cr_7C_3. Vuoristo et al. (Ref 45) and Murthy and Venkataraman (Ref 51) have also reported the formation of these phases in the HVOF-sprayed Cr_3C_2-NiCr coating. It is evident from the XRD pattern of NiCrBSi coating that the principal phase is again one with a nickel-base fcc structure with some low-intensity peaks of Ni_3B and Cr_7C_3. Similar phases have also been revealed by Dent et al. (Ref 28), Modi and Calla (Ref 29), and Miguel et al. (Ref 37) for HVOF-sprayed NiCrBSi/NiCrBC coatings. The XRD spectrum of Stellite-6 coatings shows Cobased fcc structure as the principal phase, whereas the Ni-20Cr wire coating has a principal phase of nickel-base fcc. The XRD results are further supported by EDAX analysis. The SEM observations of the presence of oxide phase in the microstructure of the coatings have been confirmed by XRD analysis. Similar findings of the presence of oxide phases in the microstructure of HVOF coatings have been reported by Dent et al. (Ref 28), Kong et al. (Ref 30), and Zhang et al. (Ref 52). The hot corrosion behavior of these

coatings in a molten salt (Na_2SO_4-60%V_2O_5) environment at 900 °C is presented in part 2 of this article.

5. Conclusions

- Cr_3C_2-NiCr, NiCrBSi, Stellite-6, and Ni-20Cr wire coatings have been successfully deposited by the HVOF-spraying process to develop coatings 250 to 300 μm thick on Fe-base superalloy substrates.
- The HVOF-sprayed coatings with given parameters have dense and uniform lamellar microstructures with porosity less than 2%. Further, a high proportion of the feedstock powders/wire appeared to have been fully or partiality melted prior to impact on the substrate surface. The SEM micrographs indicate that the coatings are free from surface/cross-sectional cracks.
- Among the coatings studied, the Cr_3C_2-NiCr coating has shown a maximum hardness in the range of 900 to 990 Hv, whereas the Ni-20Cr wire coating indicated a minimum value in the range of 595 to 630 Hv. The microhardness of the coatings is found to be higher than the superalloy. Further, the microhardness of the coatings is found to be variable with the distance from the coating-substrate interface.
- X-ray diffractograms indicate that Cr_3C_2-NiCr, NiCrBSi, and Ni-20Cr wire coatings have nickel-base fcc structure as a principal phase, whereas the Stellite-6 coating has a principal phase of Cobased fcc. An EDAX analysis of the as-sprayed coatings has indicated the formation of the required compositions of the coatings.
- Cr_2O_3 oxides and $CoNiO_2$ spinel oxides appeared in the microstructure of the Ni-20Cr and Stellite-6 coatings, respectively, in the form of either intersplat lamellae or globules. These oxides are oriented parallel to the substrate surface.

References

1. P.S. Liu, K.M. Liang, and S.R. Gu, High-temperature Oxidation Behavior of Aluminide Coatings on a New Cobalt-Base Superalloy in Air, *Corrosion Sci.,* 2001, 43, p 1217-1226
2. P.S. Sidky and M.G. Hocking, Review of Inorganic Coatings and Coating Processes for Reducing Wear and Corrosion, *Br. Corros. J.,* 1999, 34 (3), p 171-183
3. A. Matthews, R.J. Artley, and P. Holiday, Future's Bright for Surface Engineering, *Mater. World,* 1998, 6, p 346
4. W. Brandl, D. Toma, and H.J. Grabke, The Characteristics of Alumina Scales Formed on HVOF-Sprayed MCrAlY Coatings, *Surf. Coat. Technol.,* 1998, 108-109, p 10
5. L. Pawlowski, *The Science and Engineering of Thermal Spray Coatings,* Wiley, New York, 1995
6. E. Perkin, *Diamond Jet System and Gun Manual,* Metco, 1989
7. R.W. Smith and R Knight, Thermal Spraying: I. Powder Consolidation—From Coating to Forming, *J. Mater.,* 1995, 47 (8), p 32-39
8. H. Herman, S. Sampath, and R. Mccune, Thermal Spray: Current Status and Future Trends, *MRS Bull.,* 2000, 25 (7), p 17-25
9. B.Q. Wang and Z.R. Shui, The Hot Erosion Behavior of HVOF Chromium Carbide-Metal Cermet Coatings Sprayed with Different Powders, *Wear,* 2002, 253, p 550-557
10. T.S. Sidhu, R.D. Agrawal, and S. Prakash, Hot Corrosion of Some Superalloys and Role of High-Velocity Oxy-Fuel Spray Coatings: A Review, *Surf. Coat. Technol.,* 2005, 198, p 441-446
11. D.W. Parker and G.L. Kutner, HVOF-Spray Technology Poised for Growth, *Adv. Mater. Proc.,* 1991, 4, p 68
12. J.M. Guilemany, J. Fernandez, J.M. de Paco, and J. Sanchez, Corrosion Resistance of HVOF WC-Co and TiC/Ni-Ti Coatings Sprayed on Commercial Steel, *J. Surf. Eng.,* 1998, 14, p 133
13. A. Collazo, X.R. Novo, and C. Perez, Corrosion Behaviour of Cermet Coatings in Artificial Seawater, *Electrochim. Acta,* 1999, 44, p 4289
14. M. Adachi Tani, A. Nakahira, and Y. Takatani, Aqueous Corrosion Behavior of Thermally Sprayed Coatings for Steel Substrate, *Thermal Spray: Surface Engineering via Applied Research*, May 8-11, 2000 (Montréal, Québec, Canada), ASM International, 2000, p 1025
15. P. Gu, B. Arsenault, J.J. Beaudoin, J.G. Legoux, B. Harvey, and J. Fournier, Polarization Resistance of Stainless Steel-Coated Rebars, *Cem. Concr. Res.,* 1998, 28, p 321
16. A.J. Sturgeon and D.C. Buxton, The Electrochemical Corrosion Behaviour of HVOF Sprayed Coatings, *Thermal Spray: Surface Engineering via Applied Research,* May 8-11, 2000 (Montréal, Québec, Canada), ASM International, 2000, p 1011
17. D. Harvey, O. Lunder, R. Henriksen, The Development of Corrosion Resistant Coatings by HVOF Spraying, *Thermal Spray: Surface Engineering via Applied Research,* May 8-11, 2000 (Montréal, Québec, Canada), ASM International, 2000, p 991
18. A.J. Sturgeon and D.C. Buxton, High Velocity Oxy-Fuel Spraying, *T I Met Finish,* 1994, 72, p 139-140
19. M.G. Hocking, Coatings Resistant to Erosive/Corrosive and Severe Environments, *Surf. Coat. Technol.,* 1993, 62, p 460-466
20. I. Gurrappa, Identification of Hot Corrosion Resistant MCrAlY Based Bond Coatings for Gas Turbine Engine Applications, *Surf. Coat. Technol.,* 2110, 139, p 272-283
21. G.W. Goward, Overview: Protective Coatings-Purpose, Role, and Design, *Mater. Sci. Technol.,* 1986, 2, p 194-200
22. N.S. Stoloff, Wrought and P/M Superalloys, *Properties and Selection: Irons, Steels, and High-Performance,* Vol 1, ASM Handbook, 10th ed., J.R. Davis, Ed., ASM International, 1990, p 951-980
23. B.Q. Wang and K. Luer, The Erosion-Oxidation Behavior of HVOF Cr3C2-NiCr Cermet Coating, *Wear,* 1994, 174, p 177-185
24. F. Otsubo, H. Era, and K. Kishitake, Structure and Phases in Nickel-Base Self-Fluxing Alloy Coating Containing High Chromium and Boron, *J. Thermal Spray Technol.,* 2000, 91, p 107-113
25. n Riche en Nickle, *Acta Metall.,* 1987, 35 (3), p 701-710, in French
26. K.C. Antony, Wear-Resistant Cobalt-Base Alloys, *J Met.,* 1983, 39, p 52
27. P. Crook, Cobalt and Cobalt Alloys, *Properties and Selection: Non-Ferrous Alloys and Special-Purpose Materials,* Vol 2, ASM Handbook, 10th ed., ASM International, 1993, p 446
28. A.H. Dent, A.J. Horlock, D.G. McCartney, and S.J. Harris, Microstructural Characterisation of a Ni-Cr-B-C Based Alloy Coating Produced by High Velocity Oxy-Fuel Thermal Spraying, *Surf. Coat. Technol.,* 2001, 139, p 244-250
29. S.C. Modi and E. Calla, Structure and Properties of HVO Sprayed NiCrBSi Coatings, *Thermal Spray 2001: New Surfaces for a New Millennium,* C.C. Berndt, K.A. Khor, and E.F. Lugscheider, Ed., ASM International, May 28-30, 2001 (Singapore), p 281-284
30. G. Kong, D. Zhang, P.D. Brown, D.G. McCartney, and S.J. Harris, Microstructural Characterisation of High Velocity Oxy-Fuel Thermally Sprayed Stellite-6, *Mater. Sci. Technol.,* 2003, 19, p 1003-1011
31. T. Sundararajan, S. Kuroda, T. Itagaki, and F. Abe, Steam Oxidation Resistance of Ni-Cr Thermal Spray Coatings on 9Cr-1Mo Steel: Part 1. 80Ni-20Cr, *ISIJ Int.*, 2003, 43, p 95
32. T. Sundararajan, S. Kuroda, T. Itagaki, and F. Abe, Steam Oxidation Resistance of Ni-Cr Thermal Spray Coatings on 9Cr-1Mo Steel: Part 2. 50Ni-50Cr, *ISIJ Int.*, 2003, 43, p 104
33. N.F. Ak, C. Tekmen, I. Ozdemir, H.S. Soykan, and E. Celik, NiCr Coatings on Stainless Steel by HVOF Technique, *Surf. Coat. Technol.,* 2003, 173-174, p 1070-1073
34. L. Zhao, J. Zwich, and E. Lugscheider, HVOF Spraying of Al_2O_3-Dispersion-Strengthened NiCr Powders, *Surf. Coat. Technol.,* 2004, 182, p 72-77
35. A.J. Sturgeon, Microstructure Characteristics and Corrosion Behaviour of HVOF Sprayed Metallic Coatings, *Proceedings of the International Thermal Spray Conference,* Singapore, May 2001, ASM International, p 1149
36. L. Gil and M.H. Staia, Influence of HVOF Parameters on the Corrosion Resistance of NiWCrBSi Coatings, *Thin Solid Films,* 2002, 420-421, p 446-454
37. J.M. Miguel, J.M. Guilemany, and S. Vizcaino, Tribological Study of NiCrBSi Coating Obtained by Different Processes, *Tribol. Int.,* 2003, 36, p 181-187
38. M.M. Helali and M.S.J. Hashmi, A Comparative study of plasma spraying and High Velocity Oxy-Fuel (HVOF) Thermal Spraying,

Proc. of the 10th Conference of the Irish Manufacturing Committee (IMC 10), Irish Manufacturing Committee, 1992, p 377-387
39. M.E. Aalamialeagha, S.J. Harris, and M. Emamighomi, Influence of the HVOF Spraying Process on the Microstructure and Corrosion Behaviour of Ni-20%Cr Coatings, *J. Mater. Sci.,* 2003, 38, p 4587-4596
40. R.C. Tucker Jr, Chapter 11, Advanced Thermal Spray Deposition Techniques, Norwich, NY, *Handbook of Deposition Technologies for Films & Coatings*, R.F. Bunshah, Ed., William Andrew Publ./Noyes, 1994, p 591
41. C.H. Lee and K.O. Min, Effects of Heat Treatment on the Microstructure and Properties of HVOF-Sprayed Ni-Cr-W-Mo-B Alloy Coatings, *Surf. Coat. Technol.,* 2000, 132 (1), p 49-57
42. L. Gil and M.H. Staia, Microstructure and Properties of HVOF Thermal Sprayed NiWCrBSi Coatings, *Surf. Coat. Technol.,* 1999, 120-121, p 423-429
43. B. Wang and S.W. Lee, Erosion-Corrosion Behaviour of HVOF NiAl-Al_2O_3 Intermetallic-Ceramic Coating, *Wear,* 2000, 239, p 83-90
44. Y. Wang and W. Chen, Microstructures, Properties and High-Temperature Carburization Resistances of HVOF Thermal Sprayed NiAl Intermetallic-Based Alloy Coatings, *Surf. Coat. Technol.,* 2004, 183, p 18-28
45. P. Vuoristo, K. Niemi, A. Mäkelä, and T. Mäntylä, Abrasion and Erosion Wear Resistance of Cr_3C_2-NiCr Coatings Prepared by Plasma, Detonation and High-Velocity Oxyfuel Spraying, *Thermal Spray Industrial Applications,* C.C. Berndt and S. Sampath, Ed., June 20-24, 1994 (Boston, MA), ASM International, 1994, p 121-126
46. T. Sundararajan, S. Kuroda, and F. Abe, Steam Oxidation Studies on 50Ni-50Cr HVOF Coatings on 9Cr-1Mo Steel: Change in Structure and Morphology across the Coating/Substrate Interface, *Mater. Trans.,* 2004, 45 (4), p 1299-1305
47. V.H. Hidalgo, J.B. Varela, J.M. Calle, and A.C. Menendez, Characterisation of NiCr Flame and Plasma Sprayed Coatings for Use in High Temperature Regions of Boilers, *Surf. Eng.,* 2000, 16 (2), p 137-142
48. B.S. Sidhu and S. Prakash, Evaluation of the Corrosion Behaviour of Plasma-Sprayed Ni3Al Coatings on Steel in Oxidation and Molten Salt Environments at 900 °C, *Surf. Coat. Technol.,* 2003, 166, p 89-100
49. C. Verdon, A. Karimi, and J.-L. Martin, A Study of High Velocity Oxy-Fuel Thermally Sprayed Tungsten Carbide Based Coatings: Part 1. Microstructures, *Mater. Sci. Eng. A,* 1998, 246, p 11-24
50. H.M. Hawthorne, B. Arsenault, J.P. Immarigeon, J.G.Legoux, and V.R. Parameswaran, Comparison of Slurry and Dry Erosion Behaviour of Some HVOF Thermal Sprayed Coatings, *Wear,* 1999, 225-229, p 825-834
51. J.K.N. Murthy and B. Venkataraman, Abrasive Wear Behaviour of WC–CoCr and Cr_3C_2–20(NiCr) Deposited by HVOF and Detonation Spray Processes, *Surf. Coat. Technol.,* in press
52. D. Zhang, S.J. Harris, and D.G. McCartney, Microstructure Formation and Corrosion Behaviour in HVOF-Sprayed Inconel 625 Coatings, *Mater. Sci. Eng. A,* 2003, 344, p 45-56